Acta Oceanol. Sin., 2017, Vol. 36, No. 7, P. 95–101
DOI: 10.1007/s13131-017-1089-9
http://www.hyxb.org.cn
E-mail: hyxbe@263.net

Development and validation of an ocean wave retrieval algorithm for VV-polarization Sentinel-1 SAR data

LIN Bo[1], SHAO Weizeng[1]*, LI Xiaofeng[2], LI Huan[3], DU Xiaoqing[1], JI Qiyan[1], CAI Lina[1]

[1] Marine Science and Technology College, Zhejiang Ocean University, Zhoushan 316000, China

[2] Global Science and Technology, National Oceanic and Atmospheric Administration (NOAA)-National Environmental Satellite, Data, and Information Service (NESDIS), College Park, Maryland 20740, USA

[3] National Marine Data and Information Service, State Oceanic Administration, Tianjin 300171, China

Received 9 October 2016; accepted 10 January 2017

Abstract

The purpose is to study the accuracy of ocean wave parameters retrieved from C-band VV-polarization Sentinel-1 Synthetic Aperture Radar (SAR) images, including both significant wave height (SWH) and mean wave period (MWP), which are both calculated from a SAR-derived wave spectrum. The wind direction from *in situ* buoys is used and then the wind speed is retrieved by using a new C-band geophysical model function (GMF) model, denoted as C-SARMOD. Continuously, an algorithm parameterized first-guess spectra method (PFSM) is employed to retrieve the SWH and the MWP by using the SAR-derived wind speed. Forty–five VV-polarization Sentinel-1 SAR images are collected, which cover the *in situ* buoys around US coastal waters. A total of 52 sub-scenes are selected from those images. The retrieval results are compared with the measurements from *in situ* buoys. The comparison performs good for a wind retrieval, showing a 1.6 m/s standard deviation (STD) of the wind speed, while a 0.54 m STD of the SWH and a 2.14 s STD of the MWP are exhibited with an acceptable error. Additional 50 images taken in China's seas were also implemented by using the algorithm PFSM, showing a 0.67 m STD of the SWH and a 2.21 s STD of the MWP compared with European Centre for Medium-range Weather Forecasts (ECMWF) reanalysis grids wave data. The results indicate that the algorithm PFSM works for the wave retrieval from VV-polarization Sentinel-1 SAR image through SAR-derived wind speed by using the new GMF C-SARMOD.

Key words: wind speed, significant wave height, mean wave period, Sentinel-1 synthetic aperture radar

Citation: Lin Bo, Shao Weizeng, Li Xiaofeng, Li Huan, Du Xiaoqing, Ji Qiyan, Cai Lina. 2017. Development and validation of an ocean wave retrieval algorithm for VV-polarization Sentinel-1 SAR data. Acta Oceanologica Sinica, 36(7): 95–101, doi: 10.1007/s13131-017-1089-9

1 Introduction

A synthetic aperture radar (SAR) is an advanced instrument to observe the sea surface over a large area with a high spatial resolution. Satellites, which carry SAR sensors, generally operate at C-band (ERS-1/2, Envisat-ASAR, Radarsat-1/2, Sentinel-1 and Chinese GF-3), L-band (Seasat, Alos/Palsar-1/2), and X-band (TerraSAR-X with its sister TanDEM-X, Cosmo-SkyMed and Korean Kompsat-5). At present, Sentinel-1 SAR is the only free accessible data source from the available two-channel in VV- and VH-polarizations or HH- and HV-polarizations for world-wide investigator. As for the sea surface wind retrieval from C-band VV-polarization SAR data, the geophysical model functions (GMFs) of the CMOD family model are popular, e.g., CMOD4 (Stoffelen and Anderson, 1997), CMOD-IFR2 (Quilfen et al., 1998), CMOD5 (Hersbach et al., 2007) and CMOD5N (Hersbach, 2010) for a neutral wind. These GMFs were developed from ERS-1/2 SAR data and collocated wind products from scatterometer satellite or European Centre for Medium-range Weather Forecasts (ECMWF) reanalysis winds data. In fact, the CMOD family functions are applied to retrieving the wind speed from the SAR at C-band with known accuracy (Lehner et al., 1998; Monaldo et al., 2001; Yang et al., 2011; Shao et al., 2014a, b). Nevertheless, the accuracy of wind speed retrieved from VV-polarization Sentinel-1 SAR data by using CMOD5N has been investigated recently (Monaldo et al., 2016) and results show a less than 1.44 m/s standard deviation (STD) validated against wind products from scatterometer ASCAT aboard on satellite METOP-A and -B. Interestingly, another new C-band GMF for both VV- and HH-polarization, denoted as C-SARMOD, was recently proposed by Mouche and Chapron (2015). C-SARMOD for VV-polarization was refined different from previous CMOD family functions, in which the coefficients were derived from abundant Envisat-ASAR data and ASCAT winds. However, C-SARMOD has not yet been applied for wind field retrieval in the study proposed by Mouche and Chapron (2015). It is necessary to figure out that these GMFs do not work well for wind above 25 m/s due to the saturation of the backscattering signal under such wind conditions (Fernandez et al., 2006; Meissner et al., 2014; Hwang and Fois, 2015).

It is well known that tilt, hydrodynamic (Valenzuela, 1978) and velocity bunching (Alpers et al., 1981) are modulations of sea surface waves on SAR. In particular, velocity bunching is a nonlinear modulation caused by motion of the sea surface waves rel-

Foundation item: The Public Welfare Technical Applied Research Project of Zhejiang Province of China under contract No. 2015C31021; the National Key Research and Development Program of China under contract No. 2016YFC1401605; the Scientific Foundation of Zhejiang Ocean University of China.
*Corresponding author, E-mail: shaoweizeng@zjou.edu.cn

ative to satellite flight direction. As a result of that, sea surface waves shorter than specific length cannot be detected by the SAR (Alpers and Bruning, 1986) in azimuth direction (parallel to satellite flight direction is the azimuth direction; radar look direction is defined as the range direction). Therefore, ocean wave parameter retrieval, e.g., significant wave height (SWH) and mean wave period (MWP), is much more complicate than winds retrieval. A few researchers have developed theoretical-based algorithms from single-polarization SAR data such as Max-Planck Institute (MPI) (Hasselmann and Hasselmann, 1991; Hasselmann et al., 1996), semi-parametric retrieval algorithm (SPRA) (Mastenbroek and de Valk, 2000), parameterized first-guess spectra method (PFSM) (Sun and Guan, 2006; Sun and Kawamura, 2009), and partition rescaling and shift algorithm (PARSA) (Schulz-Stellenfleth et al., 2005) for ERS SAR complex data. All of these algorithms need first-guess wave spectra which is usually obtained from either numeric wave model or can be calculated from a parameterized empirical function such as Jonswap model (Hasselmann and Hasselmann, 1985). Another optional way is constructing empirical function for wave parameters without calculating a complex modulation transfer function (MTF) of each modulation, e.g., CWAVE_ERS (Schulz-Stellenfleth et al., 2007), CWAVE_ENVI (Li et al., 2011). Besides, an empirical function for SWH retrieval in hurricanes was built through studying the relation between SWH and NRCS (Romeiser et al., 2015). So far, CWAVEs have been validated for particular SAR data, e.g., ERS-2 SAR and Envisat-ASAR wave mode data at fixed angle. When CWAVEs are employed aimed to wave parameters retrieval from Sentinel-1 SAR data, the empirical model needs be refitted.

As for fully polarimetric SAR data, ocean wave retrieval algorithms were recently developed, which are based on the wave slope estimation between different band SAR images (Schuler et al., 2004; He et al., 2006; Zhang et al., 2010). However, these algorithms cannot be applied for Sentinel-1 SAR images, because Sentinel-1 SAR does not operate in fully polarimetric mode.

In this study, wind speed is retrieved from VV-polarization Sentinel-1 SAR image by using the new C-band GMF C-SARMOD. Retrieval wind speed was compared to *in situ* buoy measurements. Then, the algorithm PFSM, which has been successfully applied for wave retrieval from C- and X-band SAR data (Sun and Kawamura, 2009; Shao et al., 2015), is employed to retrieve ocean wave parameters, including both SWH and MWP, from VV-polarization Sentinel-1 SAR data. The retrieval results of the SWH and the MWP were compared with ECMWF reanalysis grids data and *in situ* buoy measurements.

The remaining part of this paper is organized as follows: the data set, including Sentinel-1 SAR data and collected wind and wave measurements from other sources, e.g., ECMWF reanalysis grids data and *in situ* buoys, are briefly described in Section 2; C-band GMFs are introduced and the retrieved wind speed by using the new GMF C-SARMOD is compared with buoy measurements and ECMWF reanalysis wind speed in Section 3; and Section 4 shows the retrieval results of the SWH and the MWP by using algorithm PFSM; conclusion is summarized in Section 5.

2 Brief description of data sets

A total of 95 VV-polarization Sentinel-1 SAR images were collected in our study. Among these images, 45 Sentinel-1 SAR imagery were acquired in StripMap mode, which covers at least one National Data Buoy Center (NDBC) buoy location provided by the National Oceanic and Atmospheric Administration (NOAA). Wind and wave were measured at interval of 10 min. In total, we have 52 matchup points acquired within 10 min. It is necessary to figure out that the wind data from *in situ* buoy were measured at 5 m height above sea surface. Hence, wind speeds were converted to values at 10 m height using the logarithmically variable wind profile,

$$\frac{U_2}{U_1} = \frac{\ln(z/z_0)}{\ln(z_m/z_0)}, \tag{1}$$

where U_2 is the wind speed at height z; U_1 is the wind speed at already known height z_m that is measured with the *in situ* buoy; and z_0 is the roughness length taken as a constant 0.000 152 employed in our previous study (Shao et al., 2014a, b). The wind rose diagram is shown in Fig. 1, in which the wind speed is at low to moderate (up to 20 m/s) and there is no indication of signal saturation problem as encountered in the application of GMF algorithms for wind retrieval. The wave rose diagram of the SWH and histogram of the MWP are shown in Fig. 2, in which the SWH is ranged from 0 to 4 m/s with a 38.9% scatter index (SI) and MWP is ranged from 3 to 10 s with a 21.1% SI.

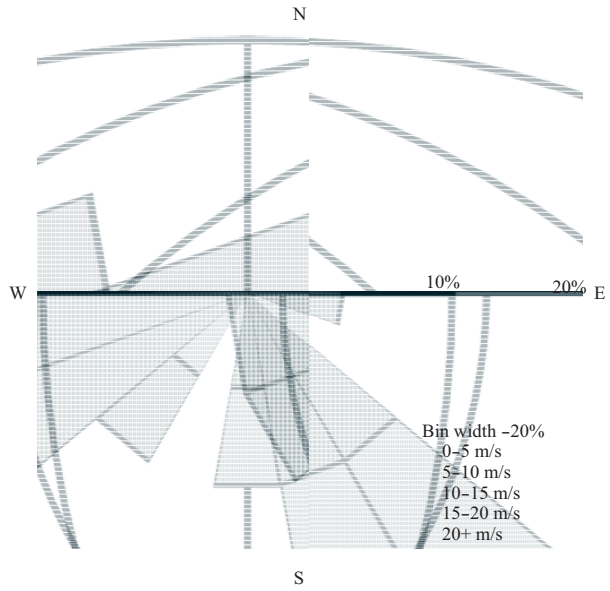

Fig. 1. Wind rose diagram of collected winds data from *in situ* buoys.

ECMWF continuously provides global reanalysis wind and wave grids data with a high spatial resolution daily at intervals of six hours since 1979. In our study, additional 50 Sentinel-1 SAR images acquired in Interferometric Wide (IW) mode were collected in China's seas, in which the time difference between SAR imaging and ECMWF reanalysis data is within three hours. As an example, the Sentinel-1 SAR image acquired 19 September 2015 at 10:16 UTC is shown in Fig. 3, in which colored arrows represent the retrieval winds by using C-SARMOD after employing the ECMWF reanalysis wind directions at a 0.5°×0.5° grid.

3 Wind speed retrieval from VV-polarization Sentinel-1 SAR data

In this section, the wind speeds were retrieved by using the new C-band GMF C-SARMOD and the results were compared with buoy measurements.

The GMF, which was designed for scatterometer, has been

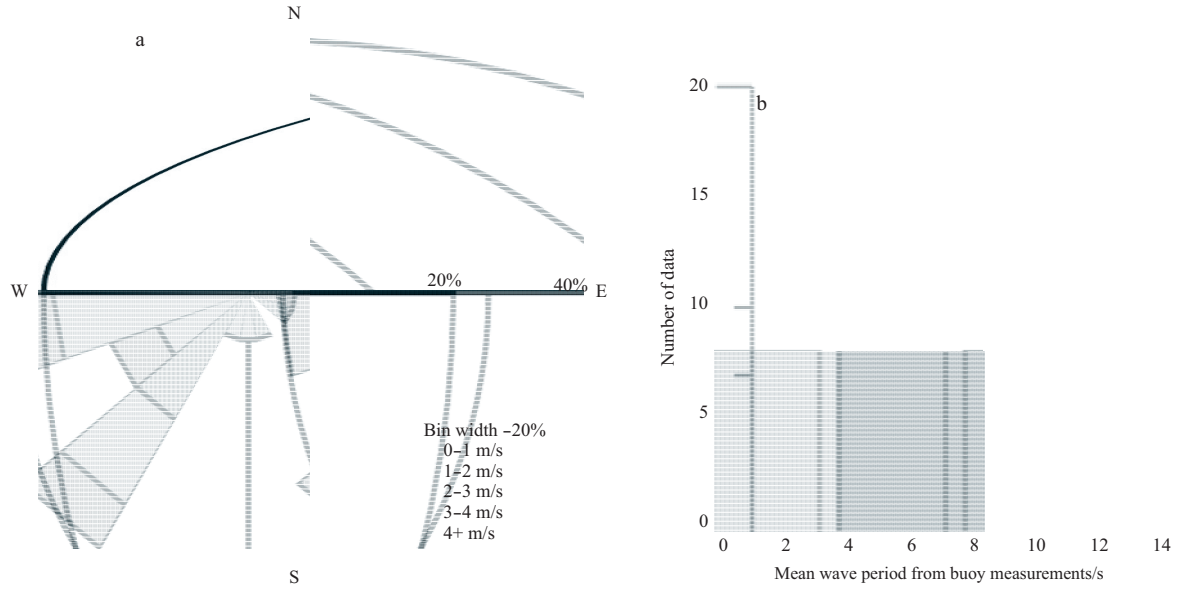

Fig. 2. Wind wave diagram of collected SWH from *in situ* buoys (a) and histogram of MWP from *in situ* buoys (b).

shown to also work for SAR data. In general, GMF relates the sea surface wind vector with radar backscattering NRCS, which take the basic formula for either traditional CMOD family models, e.g., CMOD4 (Stoffelen and Anderson, 1997), CMOD-IFR2 (Quilfen et al., 1998), CMOD5 (Hersbach et al., 2007) and CMOD5N (Hersbach, 2010) for neutral wind or the new C-SARMOD model as follows:

$$\sigma^0 = B_0(1+B_1\cos\varphi+B_2\cos 2\varphi), \tag{2}$$

where σ^0 is the SAR-measured NRCS; the coefficients B_0, B_1 and B_2 are the functions of the sea surface wind speed U_{10} and incidence angle θ; and φ is the wind direction relative to range direction. However, C-SARMOD was somehow designed different from CMOD family functions about the coefficients B_0, B_1 and B_2. Moreover, the coefficients in C-SARMOD were derived without taking into account the correction of noise equivalent σ^0 (NESZ) during Envisat-ASAR mission, which possibly distort the NRCS under low winds and the incidence angles greater than 35°.

The quick-look image from a VV-polarization Sentinel-1 SAR image on 31 December 2014 at 02:09 UTC around US coast water, is shown in Fig. 4a, as the example. Here, the ECMWF wind direction at a 0.5°×0.5° grid reanalysis data was collected over the whole image. The retrieved wind field is shown in Fig. 4b. The area, in which the center point at (46.165°N, 124.513°W) is nearest the location of the *in situ* buoy (ID: 46029) at (46.159°N, 124.414°W) corresponding to the black spot in Fig. 4a. It is found that the wind speed observed from the *in situ* buoy is 9.1 m/s, while the sea surface wind speed is 10.3 m/s with a difference of 1.2 m/s.

The accurate wind directions from *in situ* buoys were used here. Afterwards, the wind speed by using the new C-band GMF C-SARMOD were compared with measurements from *in situ* buoys. Figure 5 shows that wind speeds from all *in situ* buoy measurements versus SAR-derived wind speeds by using C-SARMOD at 2.5 m/s bins ranged from 0 to 20 m/s. The error bar represents the standard deviation (STD) of bias of each bin. Comparison shows a 1.63 m/s root mean square error (RMSE) of wind speed and a 1.6 m/s of STD. As presented in the study proposed

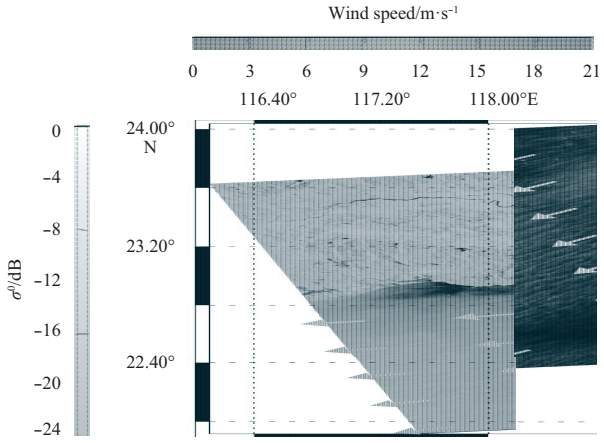

Fig. 3. A case, acquired 19 September 2015 at 10:16 UTC in China's seas, showing the quick-look image overlaid retrieval wind vectors by using C-SARMOD after employing the ECMWF wind directions at a 0.5°×0.5° grid.

by Monaldo et al. (2016), STD of wind speed by using CMOD5N is less than 1.44 m/s validated against scatterometer ASCAT wind speeds. The slight larger STD of wind speed herein is supposed to be due to different wind sources used for comparison. However, results indicate that C-SARMOD works well for wind retrieval from Sentinel-1 SAR data as well as CMOD5N and the wind speed is reliable enough to be used for wave retrieval.

4 Ocean wave parameters retrieval from VV-polarization Sentinel-1 SAR data

Theoretical-based algorithms MPI, SPRA and PFSM are often used for wave parameter retrieval from SAR data. All of them are based on the physical mechanism for the forward mapping of wave spectra into the SAR image spectra and they need first-guess wave spectra (Hasselmann and Hasselmann, 1991). In other words, the accuracy of a retrieval result depends on the accuracy of first-guess wave spectra. The simulation from numeric wave model, such as WAM (The Wamdi Group, 1988) is used in

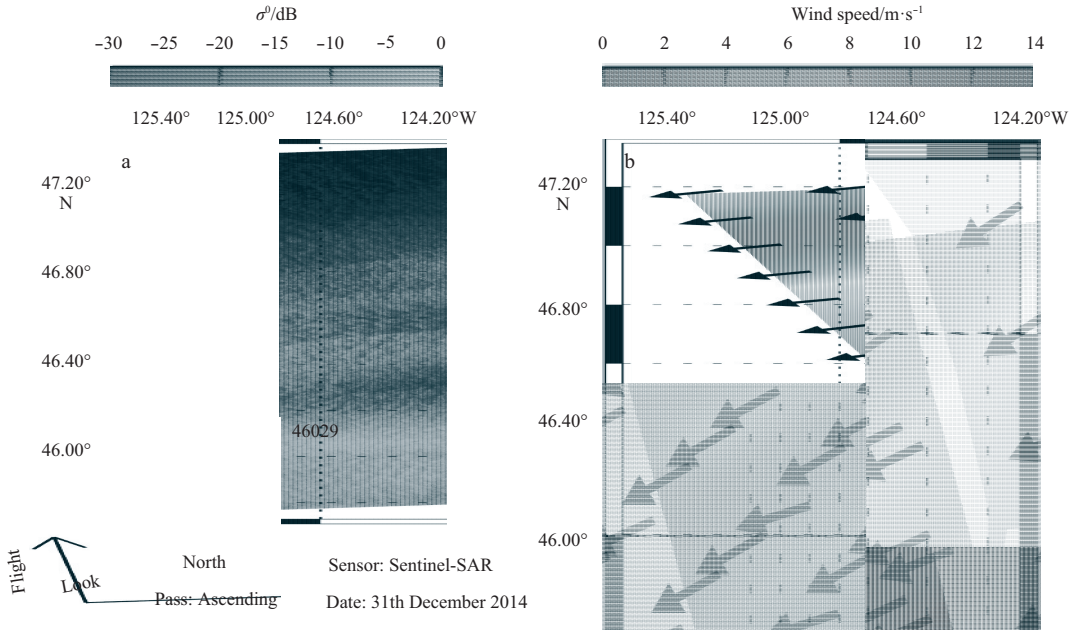

Fig. 4. A case, taken at 02:09 UTC on 31 December 2014 around US coast water, showing the quick-look image and retrieval wind vectors. a. The quick-look image and b. SAR-derived wind field. The black spot represents the location of *in situ* buoy (ID: 46029).

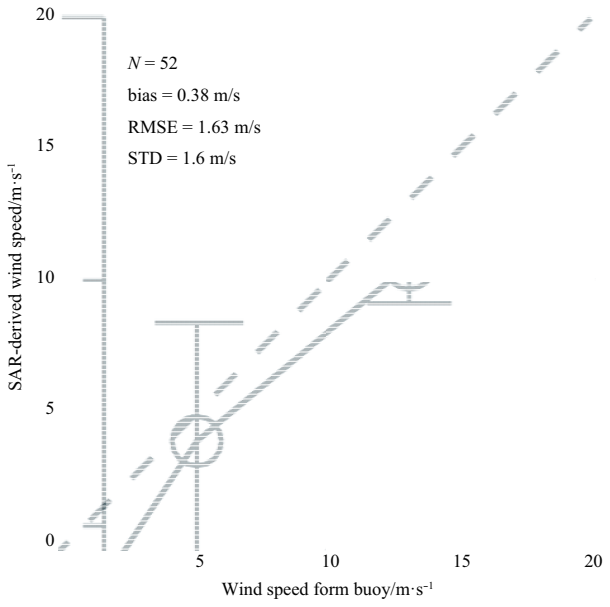

Fig. 5. SAR-derived winds speed by using C-SARMOD versus wind speeds from all *in situ* buoy at average, for 2.5 m/s of wind speed bins between 0 and 20 m/s. Error bar represents one STD after binning the comparison.

the process of MPI. SPRA method is more flexible to apply, due to it employs the computation calculated from parametric wave model, such as Jonswap empirical function (Hasselmann and Hasselmann, 1985). However, wind information from scatterometer satellite is used to produce the first-guess wave spectra in algorithm SPRA, which is not usually consistent with ocean wave on SAR in spatial and temporal scale. SAR-derived wind speed is used in algorithm PFSM. The main advantage of algorithm PFSM is that the SAR spectrum is separated into two partitions by using a threshold wave number (Sun and Guan, 2006): the local wind wave state, which represents the partition at wave number smaller than threshold wave number and the rest is classified as swell state corresponding to partition at wave number larger than threshold wave number. Moreover, it searches for the most suitable parameters of sea state, e.g., wave phase velocity and propagation direction at peak, so as to produce the best fit first-guess wind wave spectra by using a Jonswap empirical function.

After wind speed is obtained by using C-SARMOD, we use the algorithm PFSM to retrieve the one-dimensional wave spectra S_k in terms of wave number k from Sentinel-1 SAR data. Then ocean wave parameters, including SWH (H_s) and MWP (T_m), can be calculated as follows:

$$H_s = 4\sqrt{\int S_k \mathrm{d}k}\ , \tag{3}$$

$$T_m = \sqrt{\frac{\int S_k \mathrm{d}k}{\int k^2 S_k \mathrm{d}k}}\ . \tag{4}$$

As an example, the sub-scene of the VV-polarization Sentinel-1 SAR image taken on 20 October 2014 at 14:08 UTC is shown in Fig. 6a. The sub-scene covers the *in situ* buoy (ID: 46025) corresponding to the black spot and wave measurement at 14:00 UTC from the *in situ* buoy. The two-dimensional SAR spectra of sub-scene is shown in Fig. 6b and the retrieved one-dimensional wave spectra is shown in Fig. 6c. The SAR-derived SWH is 1.32 m and MWP is 4.9 s, while the SWH is 1.21 m and MWP is 6.1 s from the *in situ* buoy.

It is necessary to figure out that only the sub-scenes of the Sentinel-1 SAR image were selected for the validation in our study, in which good-quality power spectrum of NRCS can be obtained, as shown in Fig. 6b. We applied algorithm PFSM for the collected 52 sub-scenes from 45 VV-polarization Sentinel-1 SAR images so as to study the accuracy of SAR-derived SWH and

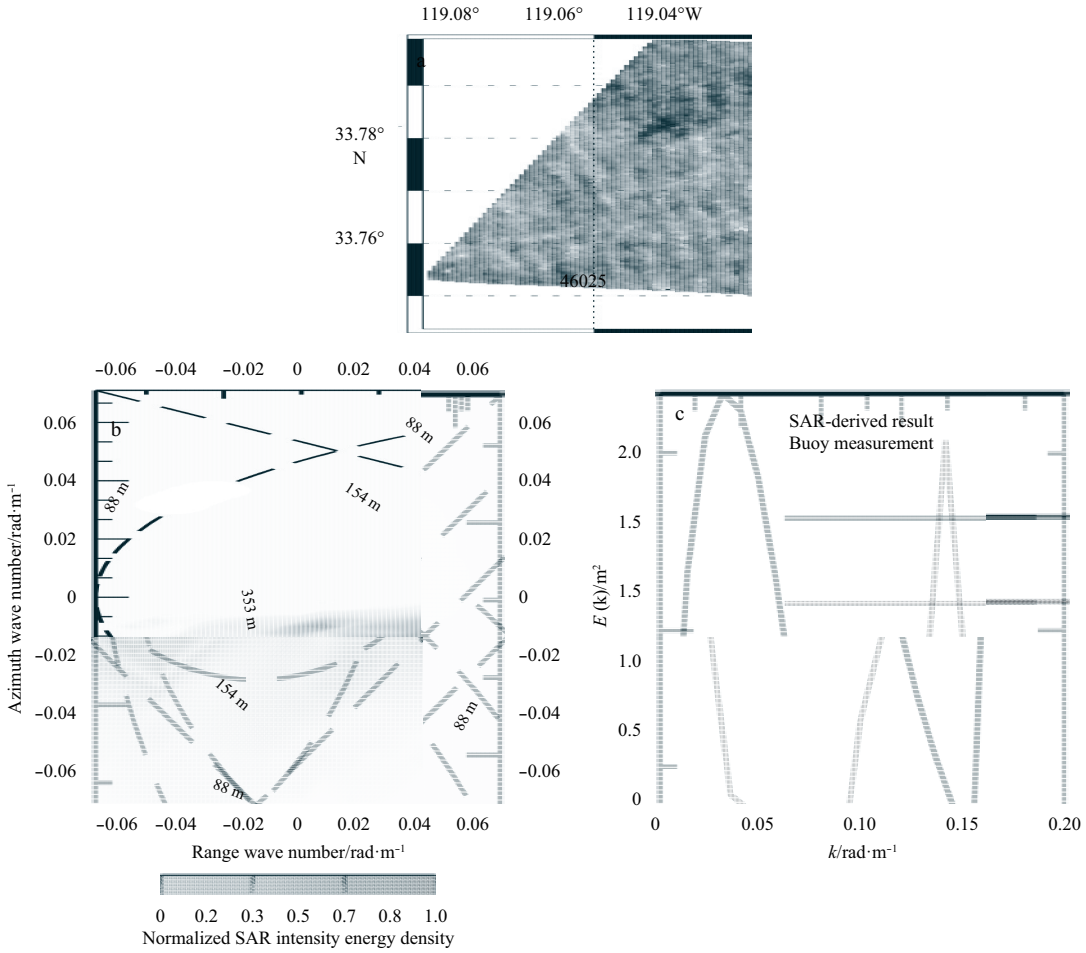

Fig. 6. The quick-look image and wave information extracted from the case acquired on 20 October 2014 at 14:08 UTC around US coast water. a. The quick-look image of the sub-scene, which covers the NDBC buoy (ID: 46025); b. the two-dimensional SAR spectra, corresponding to Fig.6a; and c. one-dimensional wave spectra retrieved by using algorithm PFSM and measured from NDBC buoy.

MWP. The retrieved results were compared to corresponding measurements from *in situ* buoys. Figure 7 shows the comparisons of the SWH and the MWP, in which the error bar represents the STD of bias of each bin, for the SWH at 0.5 m bins and the MWP at 1.5 s bins. It is shown that STD of the SWH is 0.54 m and STD of the MWP is 2.14 s. We also applied the algorithm PFSM for additional 50 Sentinel-1 SAR images in IW mode in China's seas. The sub-scenes in the images covering the ECMWF locations at a 0.5°×0.5° grids were used. Retrieval results were compared to ECMWF reanalysis wave data, showing a 0.67 m STD of the SWH at 0.5 m bins with a 2.21 s STD of the MWP at 1.5 s bins, as exhibited in Fig. 8. The herein statistical result performs somehow worse than the result shown in Fig. 7, we think it is probably caused due to coarse temporal resolution of ECMWF reanalysis data.

Referred to achievement of several researches for the wave retrieval from the SAR data, The STD of retrieved SWH with respect to the results from a numeric WAM model or *in situ* buoy measurements is less than 0.7 m. Therefore, we think the algorithm PFSM can be applied for the wave retrieval from VV-polarization Sentinel-1 SAR data, as showing a less 0.65 m STD of the retrieval SWH validated against *in situ* buoys and the ECMWF reanalysis wave data.

5 Conclusions

A tuned GMF is often used for wind retrieval from the SAR data. CMOD family functions were developed from the NRCS from VV-polarization ERS-1/2, and collocated winds from scatterometer and the ECMWF reanalysis wind fields. The new GMF C-SARMOD was derived from Envisat-ASAR data in VV-polarization and it was designed different from previous CMOD family functions. In this study, we collected a total of 52 sub scenes from 45 VV-polarization Sentinel-1 SAR images, which all cover the NOAA buoys. The retrieval wind speeds by using the C-SARMOD were compared with the measurements from *in situ* buoys. The results show that the STD of the wind speed is 1.6 m/s.

The algorithm PFSM was employed to retrieve SWH and MWP. As an example, the case study using the VV-polarization Sentinel-1 SAR image acquired on 20 October 2014 is shown in Fig. 6. In total, 52 sub-scenes from Sentinel-1 SAR images covering *in situ* buoys were selected to validate the algorithm PFSM. It was found that the STD of the SWH is 0.54 m and the STD of the MWP is 2.14 s. Moreover, additional 50 images acquired in IW mode in China's seas were implemented and the retrieval results were compared to the ECMWF reanalysis wave data, showing a 0.67 m STD of the SWH and a 2.21 s STD of the MWP.

In summary, although the results indicate the new GMF C-SARMOD works for wind retrieval as well as CMOD5N and the algorithm PFSM is suitable for wave parameter retrieval from VV-polarization Sentinel-1 SAR image, the bias existing in algorithm PFSM can be further investigated through collecting more Sen-

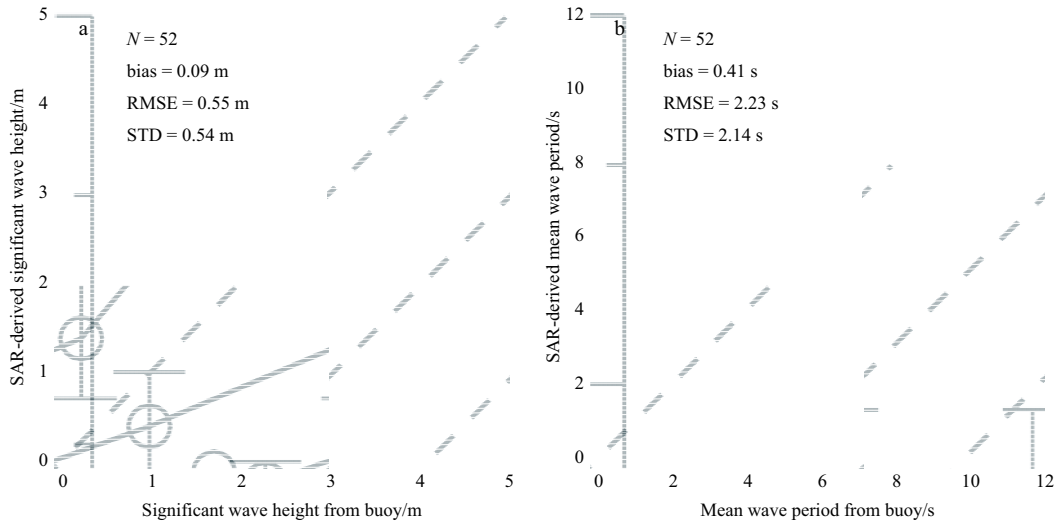

Fig. 7. SAR-derived ocean wave parameter by using algorithm PFSM versus measurements from *in situ* buoys at average. a. The SWH comparison at 0.5 m bins between 0 and 4 m, b. the MWP comparison at 1.5 s bins between 3 and 10 s. Error bar represents the STD of bias of each bin.

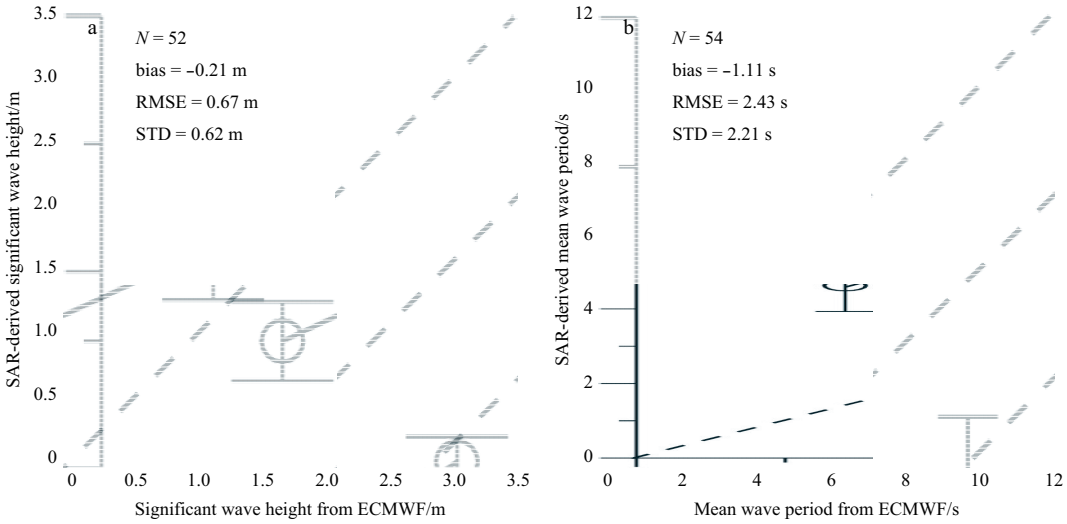

Fig. 8. SAR-derived ocean wave parameter by using algorithm PFSM versus ECMWF reanalysis wave data at average. a. The SWH comparison at 0.5 m bins between 0 and 3.5 m, and b. the MWP comparison at 1.5 s bins between 1 and 10 s. Error bar represents the STD of bias of each bin.

tinel-1 images matchup with moored measurements in the future. As for wind retrieval from HH-polarization SAR data, the combining method, that is GMF together with polarization ratio (PR) model, is usually used. Various PR models, involving only incidence angle, were developed (Thompson et al., 1998; Vachon and Dobson, 2000; Horstmann et al., 2000; Wackerman et al., 2002; Monaldo et al., 2001). Another PR model, involving both incidence angle and wind direction, was proposed by Mouche et al. (2005). These PR models have been applied for the wind retrieval from HH-polarization Sentinel-1 SAR data. It was found that CMOD4 plus PR model proposed by Thompson et al. (1998) is the best combination (Monaldo et al., 2016). We plan to apply HH-polarization C-SARMOD for wind retrieval from HH-polarization Sentinel-1 SAR data. Further, we can study the accuracy of retrieved SWH and MWP by using algorithm PFSM from HH-polarization Sentinel-1 SAR image.

Acknowledgements

The authors appreciate the European Space Agency to provide freely accessible Sentinel-1 SAR images through https://scihub.copernicus.eu. The wind and wave measurements from *in situ* buoy were collected at http://www.ndbc.noaa.gov/. ECMWF reanalysis wind and wave data were openly accessed from http://www. ecmwf.int. The views, opinions, and findings contained in this paper are those of the authors and should not be construed as an official NOAA or US Government position, policy or decision.

References

Alpers W R, Bruning C. 1986. On the relative importance of motion-related contributions to the SAR imaging mechanism of ocean surface waves. IEEE Transactions on Geoscience and Remote Sensing, GE-24(6): 873–885

Alpers W R, Ross D B, Rufenach C L. 1981. On the detectability of

ocean surface waves by real and synthetic aperture radar. Journal of Geophysical Research, 86(C7): 6481–6498
Fernandez D E, Carswell J R, Frasier S, et al. 2006. Dual-polarized C- and Ku-band ocean backscatter response to hurricane-force winds. Journal of Geophysical Research, 111(C8): doi: 10.1029/2005JC003048
Hasselmann S, Brüning C, Hasselmann K, et al. 1996. An improved algorithm for the retrieval of ocean wave spectra from synthetic aperture radar image spectra. Journal of Geophysical Research, 101(C7): 16615–16629
Hasselmann S, Hasselmann K. 1985. Computations and parameterizations of the nonlinear energy transfer in a gravity-wave spectrum: I. a new method for efficient computations of the exact nonlinear transfer integral. Journal of Physical Oceanography, 15(11): 1369–1377
Hasselmann K, Hasselmann S. 1991. On the nonlinear mapping of an ocean wave spectrum into a synthetic aperture radar image spectrum and its inversion. Journal of Geophysical Research, 96(C6): 10713–10729
He Yijun, Shen Hui, Perrie W. 2006. Remote sensing of ocean waves by polarimetric SAR. Journal of Atmospheric and Oceanic Technology, 23(12): 1768–1773
Hersbach H. 2010. Comparison of C-band scatterometer CMOD5. N equivalent neutral winds with ECMWF. Journal of Atmospheric and Oceanic Technology, 27(4): 721–736
Hersbach H, Stoffelen A, Haan S D. 2007. An improved C-band scatterometer ocean geophysical model function: CMOD5. Journal of Geophysical Research, 112(C3): doi: 10.1029/2006JC003743
Horstmann J, Koch W, Lehner S, et al. 2000. Wind retrieval over the ocean using synthetic aperture radar with C-band HH polarization. IEEE Transactions on Geoscience and Remote Sensing, 38(5): 2122–2131
Hwang P A, Fois F. 2015. Surface roughness and breaking wave properties retrieved from polarimetric microwave radar backscattering. Journal of Geophysical Research, 120(5): 3640–3657
Lehner S, Horstmann J, Koch W, et al. 1998. Mesoscale wind measurements using recalibrated ERS SAR images. Journal of Geophysical Research, 103(C4): 7847–7856
Li Xiaoming, Lehner S, Bruns T. 2011. Ocean wave integral parameter measurements using envisat ASAR wave mode data. IEEE Transactions on Geoscience and Remote Sensing, 49(1): 155–174
Mastenbroek C, de Valk C F. 2000. A semiparametric algorithm to retrieve ocean wave spectra from synthetic aperture radar. Journal of Geophysical Research, 105(C2): 3497–3516
Meissner T, Wentz F J, Ricciardulli L. 2014. The emission and scattering of L-band microwave radiation from rough ocean surfaces and wind speed measurements from the Aquarius sensor. Journal of Geophysical Research, 119(9): 6499–6522
Monaldo F M, Jackson C, Li Xiaofeng, et al. 2016. Preliminary evaluation of sentinel-1A wind speed retrievals. IEEE Journal of Selected Topics in Applied Earth Observations and Remote Sensing, 9(6): 2638–2642
Monaldo F M, Thompson D R, Beal R C, et al. 2001. Comparison of SAR-derived wind speed with model predictions and ocean buoy measurements. IEEE Transactions on Geoscience and Remote Sensing, 39(12): 2587–2600
Mouche A A, Chapron B. 2015. Global C-band envisat, RADARSAT-2 and sentinel-1 SAR measurements in copolarization and cross-polarization. Journal of Geophysical Research, 120(11): 7195–7207
Mouche A A, Hauser D, Daloze J F, et al. 2005. Dual polarization measurements at C-band over the ocean: results from airborne radar observations and comparison with ENVISAT ASAR data. IEEE Transactions on Geoscience and Remote Sensing, 43(4): 753–769
Quilfen Y, Chapron B, Elfouhaily T, et al. 1998. Observation of tropical cyclones by high-resolution scatterometry. Journal of Geophysical Research, 103(C4): 7767–7786
Romeiser R, Graber H C, Caruso M J, et al. 2015. A new approach to ocean wave parameter estimates from C-band ScanSAR images. IEEE Transactions on Geoscience and Remote Sensing, 53(3): 1320–1345
Schuler D L, Lee J S, Kasilingam D, et al. 2004. Measurement of ocean surface slopes and wave spectra using polarimetric SAR image data. Remote Sensing of Environment, 91(2): 198–211
Schulz-Stellenfleth J, König T, Lehner S. 2007. An empirical approach for the retrieval of integral ocean wave parameters from synthetic aperture radar data. Journal of Geophysical Research, 112(C3): doi: 10.1029/2006JC003970
Schulz-Stellenfleth J, Lehner S, Hoja D A. 2005. A parametric scheme for the retrieval of two-dimensional ocean wave spectra from synthetic aperture radar look cross spectra. Journal of Geophysical Research, 110(C5): doi: 10.1029/2004JC002822
Shao Weizeng, Li Xiaoming, Lehner S, et al. 2014a. Development of polarization ratio model for sea surface wind field retrieval from TerraSAR-X HH polarization data. International Journal of Remote Sensing, 35(11): 4046–4063
Shao Weizeng, Li Xiaofeng, Sun Jian. 2015. Ocean wave parameters retrieval from TerraSAR-X images validated against buoy measurements and model results. Remote Sensing, 7(10): 12815–12828
Shao Weizeng, Sun Jian, Guan Changlong, et al. 2014b. A method for sea surface wind field retrieval from SAR image mode data. Journal of Ocean University of China, 13(2): 198–204
Stoffelen A, Anderson D. 1997. Scatterometer data interpretation: estimation and validation of the transfer function CMOD4. Journal of Geophysical Research, 102(C3): 5767–5780
Sun Jian, Guan Changlong. 2006. Parameterized first-guess spectrum method for retrieving directional spectrum of swell-dominanted waves and huge waves from SAR images. Chinese Journal of Oceanology and Limnology, 24(1): 12–20
Sun Jian, Kawamura H. 2009. Retrieval of surface wave parameters from SAR images and their validation in the coastal seas around Japan. Journal of Oceanography, 65(4): 567–577
The Wamdi Group. 1988. The WAM model-a third generation ocean wave prediction model. Journal of Physical Oceanography, 18(12): 1775–1810
Thompson D R, Elfouhaily T M, Chapron B. 1998. Polarization ratio for microwave backscattering from the ocean surface at low to moderate incidence angles. In: 1998 IEEE International Geoscience and Remote Sensing Symposium Proceedings. Vol 3. Seattle, WA: IEEE, 1671–1673
Vachon P W, Dobson F W. 2000. Wind retrieval from RADARSAT SAR images: selection of a suitable C-band HH polarization wind retrieval model. Canadian Journal of Remote Sensing, 26(4): 306–313
Valenzuela G R. 1978. Theories for the interaction of electromagnetic and oceanic waves-a review. Boundary-Layer Meteorology, 13(14): 61–85
Wackerman C C, Clemente-Colón P, Pichel W G, et al. 2002. A two-scale model to predict C-band VV and HH normalized radar cross section values over the ocean. Canadian Journal of Remote Sensing, 28(3): 367–384
Yang Xiaofeng, Li Xiaofeng, Zheng Quanan, et al. 2011. Comparison of ocean-surface winds retrieved from quikSCAT scatterometer and radarsat-1 SAR in offshore waters of the US west coast. IEEE Geoscience and Remote Sensing, 8(1): 163–167
Zhang Biao, Perrie W, He Yijun. 2010. Validation of RADARSAT-2 fully polarimetric SAR measurements of ocean surface waves. Journal of Geophysical Research, 115(C6): doi: 10.1029/2009JC005887